Validation of the pyramid tracing algorithm for sound propagation outdoors: comparison with experimental measurements and with the ISO/DIS 9613 standards

A. Farina
Department of Industrial Engineering, University of Parma,
Via delle Scienze, I-43100 PARMA, Italy
tel. +39 0521 905854 - fax 905705 - E-MAIL farina@pcfarina.eng.unipr.it –
HTTP://pcfarina.eng.unipr.it

Abstract
The aim of this work is to test the accuracy of numerical previsions of the sound propagation outdoors made with the newly developed pyramid tracing algorithm [1,2]. Pyramid tracing has already been proposed and validated for indoor calculation, both for the study of the sound quality in concert halls or other Sabinian spaces, and for noise reduction in factories or other non Sabinian spaces [3,4].

As the algorithm allows for the evaluation of sound passing through sound insulating panels, taking also into account the edge diffraction over free boundaries of screens, it is natural that it can be used also for the simulation of sound propagation outdoors.

Anyway it must be noted that the actual implementation of pyramid tracing, available in the Ramsete package, does not take into account the interference effects caused by propagation at grazing incidence over the soil, neither the ray curvature caused by temperature or air velocity vertical gradients.

In this paper a comparative experiment is described, in which the pyramid tracing code was tested against experimental measurements (made with an innovative Maximum Length Sequence signal, previously used only for room acoustics). The sound source was a directive loudspeaker, which Sound Power Levels and Directivity Balloons in Octave Bands were previously measured in free field conditions. The measurement in each point was obtained through asynchronous cross-correlation of the signal coming from a standard Sound Level Meter (recorded for convenience on a DAT tape recorder) and the original MLS sequence, through a fast-Hadamard algorithm, yielding the Impulse Response between the Source and the Receiver positions. With proper synchronous averaging of the incoming signal, a great improvement in the Signal-To-Noise Ratio was achieved, making it possible to make measurements almost not affected by background noise even in highly shielded positions.
The comparison is made also with an Image Source code, built up around the computing formulas contained in the new ISO-DIS standard 9613, kindly made available by Luigi Maffei [5]

The test case was chosen in an area containing all the most interesting acoustic phenomena: large distance propagation over absorbing and reflecting soil, shielding by embankments and buildings, multiple reflections on buildings facades. Only adverse atmospheric conditions were not taken into account (strong wind, inverted temperature gradient).

Both the experimental and numerical data were used to build graphical plots, enabling a direct comparison of the results: they show that the capability of accurately modeling the source directivity produce generally a better estimate using the pyramid tracing algorithm, but the shielding effects and excess attenuation are more accurately modeled by the ISO9613 code.

1. The Pyramid Tracing model

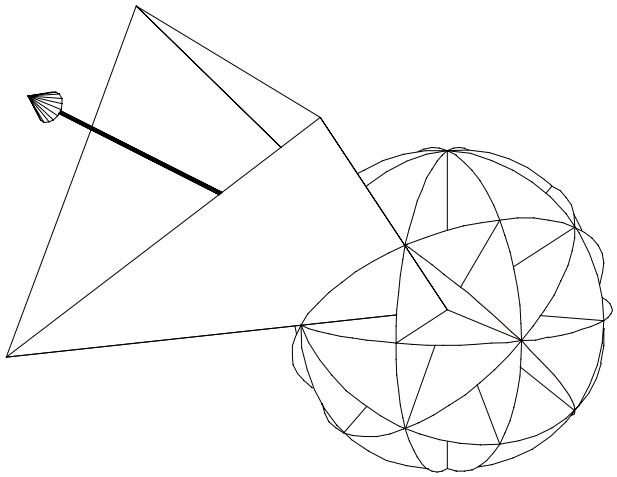

Figure 1 - subdivision of the source's surface in triangular beams

Ramsete is one of the first pyramid tracing codes that was developed for room acoustic simulations. At the time of its first appearance (1993) [6,7], only the work of Lewers [8] reported a "triangular beam tracing" hybrid method.

In the Pyramid Tracing scheme, triangular beams are generated at the sound source, as shown in fig. 1. The central axis of each pyramid is traced as usual, being specularly reflected when it hits on a surface. The three corners of the pyramid follow the axis, being reflected from the same plane where it hits, also if the intersection point is outside the facet where the axis hits (non-splitting-up pyramid tracing).

The receivers are points, and a detection occurs when this point is inside the pyramid being traced. In this case, a pseudo-intensity contribution I' is recorded (along with the time elapsed since pyramid emission) for each octave band:

$$I' = \frac{P_{wr} \cdot Q_{\vartheta} \cdot \prod_i (1-\alpha_i)}{4 \cdot \pi \cdot x^2} \cdot e^{-\gamma \cdot x} \qquad (1)$$

in which x is path length, γ is the absorption coefficient of air, Q_θ is the directivity factor and P_{wr} is the acoustic power of the source. The computation is made in 10 octave bands.

Ramsete is not an hybrid model: the tracing of pyramids is prosecuted up to the whole time length required to analyse the impulse response, and no point of transition exists between the "early" part of the decay and the "late" one. The author already published the details of the tail correction algorithm (Farina [1]).

For the purposes of the present work, it is necessary to recall here the meaning of the two numerical parameters α and β, the value of which needs to be adjusted to model non-Sabinian (enclosed) spaces with a little number of pyramids.

α: is the exponent to be applied to the current time, to find the number of reflected waves arriving to a receiver in the time unit (usually called temporal echo density). For example, in Sabinian room α=2, in a tunnel-like room it approaches 1, while in a very low room (only 2 counterpoised surfaces) the temporal echo density is constant, so the exponent α is 0. In some cases α can also be very greater than 2.

β: is a coefficient inserted in the formula for calculating the **critical time t_c**: this is defined as the time at which the "true" temporal echo density (that usually increases with time) is equal to the "false" constant echo density produced by the pyramid tracing (that is simply proportional to the number of pyramids, and inversely proportional to the mean free path). The parameter β

can adjust t_c from infinity (no correction, β=0, as it is proper for outdoors) to the Sabinian value (β=0.1) [1].

Another point which needs to be explained here is the capability to treat "holed" and "obstructing" surfaces, as this greatly speeds up the program. Usual surfaces are quadrilateral plane faces, defined by the co-ordinates of their vertexes. If they are declared "obstructing", additional tests are made to find the sound attenuation of pyramids "passing through" the panel and being diffracted from its free edges (automatically located). On a surface it is also possible to "attach" three types of entities: doors, windows and holes. Doors and windows are rectangular areas, having absorption coefficients and sound reduction indexes different from that of the wall. The holes are closed polylines, that define regions where the pyramids can freely pass through an obstructing wall.

These features produce a noticeable reduction in computing time, as the number of (main) surfaces is reduced, and the complete set of tests is conducted on the "obstructing" surfaces only. Figure 2 shows an example (from Ramsete Cad) of these modelling capabilities.

Although Ramsete is not a Montecarlo method, still a convergence to the "right" values can be seen increasing the number of pyramids traced: introducing proper values of coefficients α and β makes it possible to obtain correct results using just 256 pyramids or even less, with computations times reduced to a couple of minutes for each sound source in the worst cases.

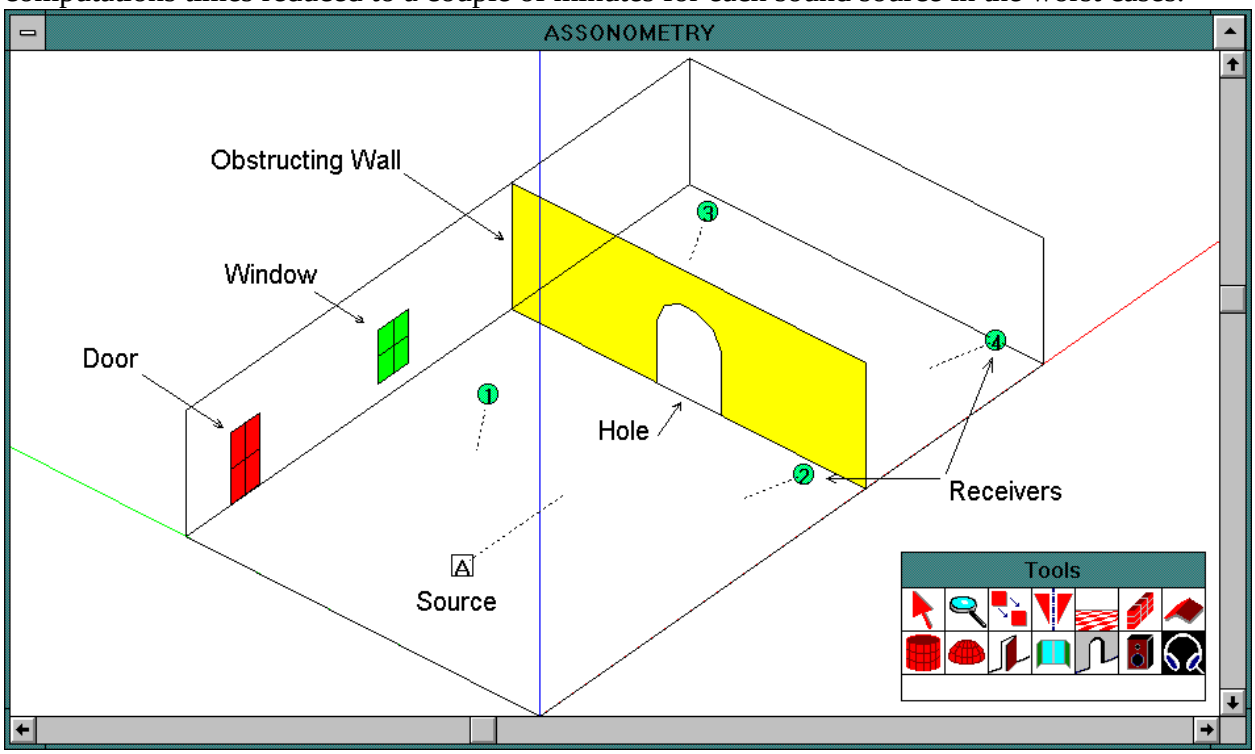

Figure 2 - Advanced Surface Attributes in Ramsete

It must be noted, however, that in outdoors propagation there is not any reverberant tail to be "corrected", and that a large number of pyramids can be used with very little computation times, as most of them are "lost" after a little number of reflections: so there are not, in general, "missing" image sources as it happens in indoor cases, and the tail correction parameters are not influent on the results.

Besides the particularities of the pyramid tracer, it must also be noted that the program

comes with an innovative Source Manager [7]: it manages the source directivities and sound power data files, and makes it possible to automatically define directivity balloons (with standard 10° by 10° resolution) from experimental measurements conducted according to ISO standards 3744 and 3746, with direct reading of the most common Real Time Analyser file formats. This is particularly important for the noise sources, for which no directivity data are usually collected. However the program easily imports also the loudspeaker directivity data stored in the Bose Modeler (TM) and EASE (TM) format.

The algorithm contains also proper extensions to take into account shielding effects and excess attenuation, that are discussed here. The evaluation of the sound energy diffracted from the free edges of a screen is made using the well-known Kurze formula [9]:

$$L_{diff} = L_{dir} - 5 - 20 \cdot \lg\left(\frac{\sqrt{2 \cdot \pi \cdot |N|}}{\tanh \sqrt{2 \cdot \pi \cdot |N|}} \right) \qquad (2)$$

in which L_{dir} is the Direct Level, that should arrive to the receiver if the screen were not in place, and N is the Fresnel number, given as:

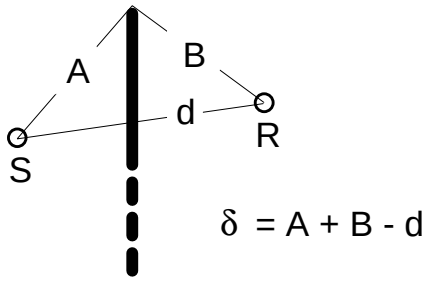

$$N = \frac{2}{\lambda} \cdot \delta = \frac{2 \cdot f}{c} \cdot \delta \qquad (3)$$

When a surface is declared “obstructing” in the input data file, a check is made for finding its free edges. For each free edge found, an energy contribution to the receiver is calculated with the above formulas, plus the energy passing “through” the panel (reduced of its sound reduction index): this happens both for the direct wave, both for the reflected ones. Furthmore, the code does check for double diffractions, as shown in fig. 3:

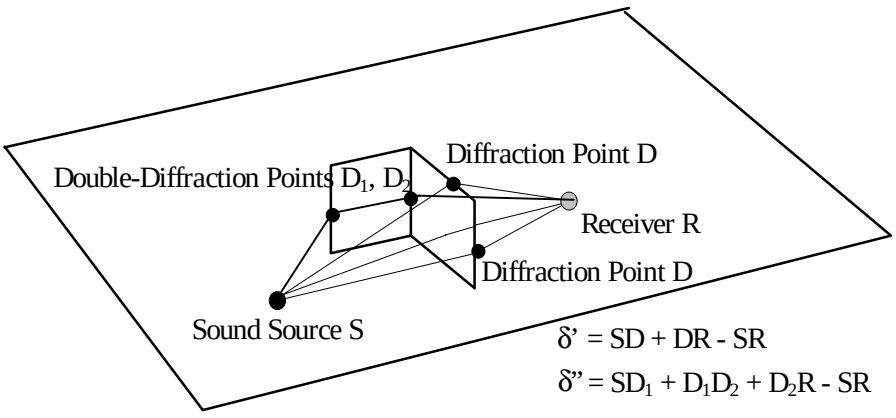

Figure 3 - Free Edge diffractions plus energy passing through the panel

The other great problem in outdoor propagation is the excess attenuation. It is known that it results from many different phenomena: air absorption, grazing incidence over the absorbing soil, interference between the direct field and the reflected one over reflecting soil, ray curvature due to wind or temperature gradients.

Only the first effect (air absorption) is taken into account in Ramsete, and only with a simplified formulation: in fact, Sound Energy Density W is reduced during the propagation by multiplicating for an exponential extinction term, as already shown in eq. (1), and the frequency-dependent extinction coefficient γ is computed taking into account only the percent relative humidity of the air $\varphi_{\%}$ (0-100):

$$\gamma = \frac{1.7 \cdot 10^{-8} \cdot f^2}{\varphi_{\%}} \tag{4}$$

No other excess attenuation term is actually included in Ramsete, although it could be advisable in the future to include ray curvature and ground-effect in the computation, employing simplified mathematical formulation of these effects, as suggested in [10].

All the input data must be introduced in the 10 octave bands from 31.5 Hz to 16 kHz: Power Levels and Directivity Balloons of the sources, absorption coefficients and sound reduction indexes of surfaces. The computations are made for each octave band, and then the overall Lin and A-weighted Sound Pressure Level are post-computed.

2. Image Sources code following ISO 9613

The new ISO-DIS 9613 (parts 1 and 2) standard contains a detailed method for computing the sound propagation outdoors, taking into account also the effects caused by the propagation over soil with varying properties, shielding both from thin and thick obstacles, effects of vegetation layers, excess attenuation. In particular, the air absorption is treated with great detail: the whole part 1 of the standard covers this only point.

The sound level at the receiving point is calculated with the following formula (ISO 9613/2):

$$L_{rec} = L_w + 10 \cdot \lg\left(\frac{Q}{4 \cdot \pi \cdot d^2}\right) - A_{air} - A_{ground} - A_{screen} - A_{refl} - A_{misc} \tag{5}$$

The (quite complex) expressions for the attenuation terms in eqn (5) are not reported here, as they are part of an ISO standard. However, some detail is needed to understand the implementation of that equation in an automated computing code, as the one developed by Maffei and used here for comparison.

Each sound source is introduced simply by its Cartesian co-ordinates, followed by the Sound Power Levels in octave bands from 63 Hz to 8 kHz and Directivities in dB (= 10·logQ).

The soil is divided in homogeneous quadrilateral areas, described by their X-Y co-ordinates (only flat land areas are considered for now): the soil can be only classified as “hard” , “soft” or “very soft”.

Vertical reflecting surfaces (walls, screens, etc.) are introduced by the co-ordinates of their upper edge: these surfaces are characterised by absorption coefficients in octave bands.

It is possible also to introduce dense foliage volumes, as quadrilateral areas with a fixed height. By the same technique it is possible to introduce areas with partial building coverage or other partially obstructed volumes.

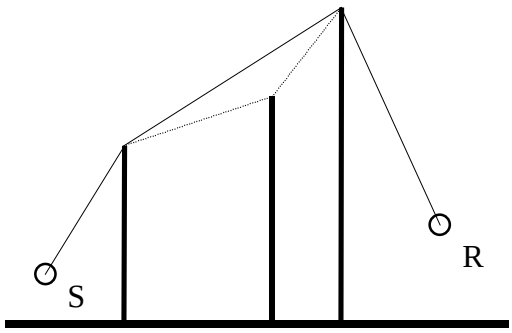

Figure 4 - Determination of the diffracted path with multiple screens

The computation algorithm automatically locates the soil area covered by the rays, and identifies any potentially diffracting edge (horizontal or vertical). A check is made also for multiple diffractions, discarding non-relevant edges by a minimum-distance technique, as shown from figure 4:

The reflections over vertical surfaces (giving "negative" attenuation A_{refl}) are taken into account generating the image source for each vertical surface, and checking it for visibility "through" the area of the surface itself. A further check is made to discard image sources shielded by other vertical surfaces, but in this case no further diffraction computation is made, and the energy that comes from a reflection followed by a diffraction is completely neglected.

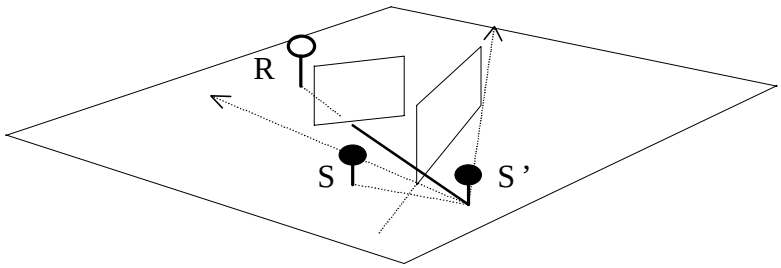

Figure 5 - Visibility check of an Image Source

3. Experimental Measurements

An innovative measuring technique was used to collect experimental data with little background noise contamination. It is based on the mathematical properties of the MLS (Maximum Length Sequence) excitation signal, as suggested by Chu for room acoustics measurements [11].
A small loudspeaker is fed, through a battery operated power amplifier, with the steady MLS signal produced by a MLSSA A/D board installed in a portable, battery operated computer. The measuring device is a sound level meter, with a DAT recorder connected to its calibrated AC output; this way no connection exist between the signal generator and the recording device.

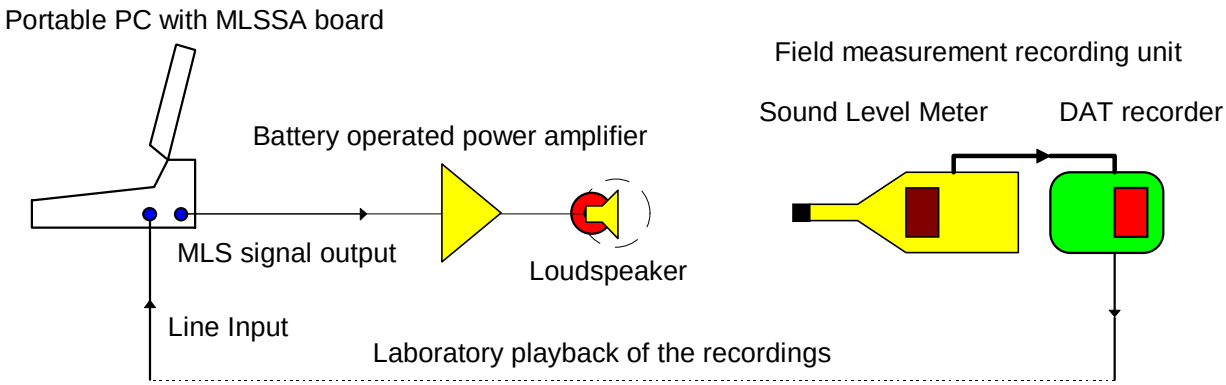

Fig. 6 - Sketch of the measuring system

After the recordings have been made in all the measuring points, the DAT recorder output is connected with the input of the MLSSA board, and through asynchronous cross correlation of the recorded signal with the original MLS, the impulse response between source and receiver is recovered. The recordings are calibrated, so "true" SPL values can be measured in octave bands with the post processing tools of the MLSSA software. However a check on the overall SPL shown on the S.L.M. display was always successfully made, showing maximum difference of 0.3 dB.

The reliability of asynchronous MLS measurements by use of a portable, consumer-level DAT recorder was recently investigated by Chu [12], who found that in 50 cases out of 60 this technique produces Sound Pressure Level measurements within the precision of type-1 instrumentation (indoor). It is possible that outdoors the propagation conditions are much more unstable, so that the MLS excitation signal could behave less well than indoors. As the employ of the MLS signal for outdoor measurement is completely new, it was not possible to find any relevant paper which discusses this point.

The MLS measurements are inherently immune from background noise, because the cross-correlation process gives a S/N improvement of nearly 30 dB against traditional "real-time" measurements. Furthermore, a synchronous pre-averaging of 16 consecutive samples was performed on the raw data (prior of deconvolution of the impulse response), giving another 12 dB improvement of the S/N ratio. With this technique, any background contamination was avoided at frequencies of 125 Hz and up. At the lower frequency bands (31.5 and 63 Hz), some background noise was visible in the points located vary far from the source, but this was not caused from the MLS measuring system, but from the sound source, that was very inefficient at these low frequencies.

Figure 7 shows the source characteristics as Sound Power Spectrum and as Directivity curves. As the source is perfectly axisimmetrical, just one plane of directivity was needed to completely characterise its directivity balloon.

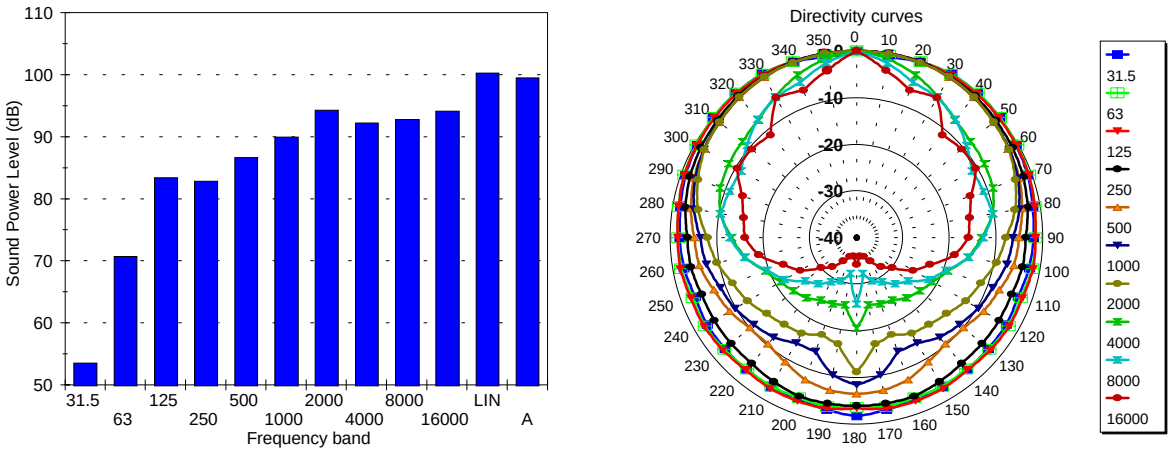

Figure 7 - Power Levels (with white noise) and Directivity of the Sound Source

3.1 Test Case

The measurements were performed at the University Campus of Parma, in an empty car park and between the buildings of the Faculty of Engineering. In figure 8 (actually it is a printout of the Ramsete Cad model) it is possible to see the source position (labelled "A") and the 16 microphone positions, placed on a straight line and spaced 10m each other. The source axis was pointed towards the buildings, being parallel to the measurement line.

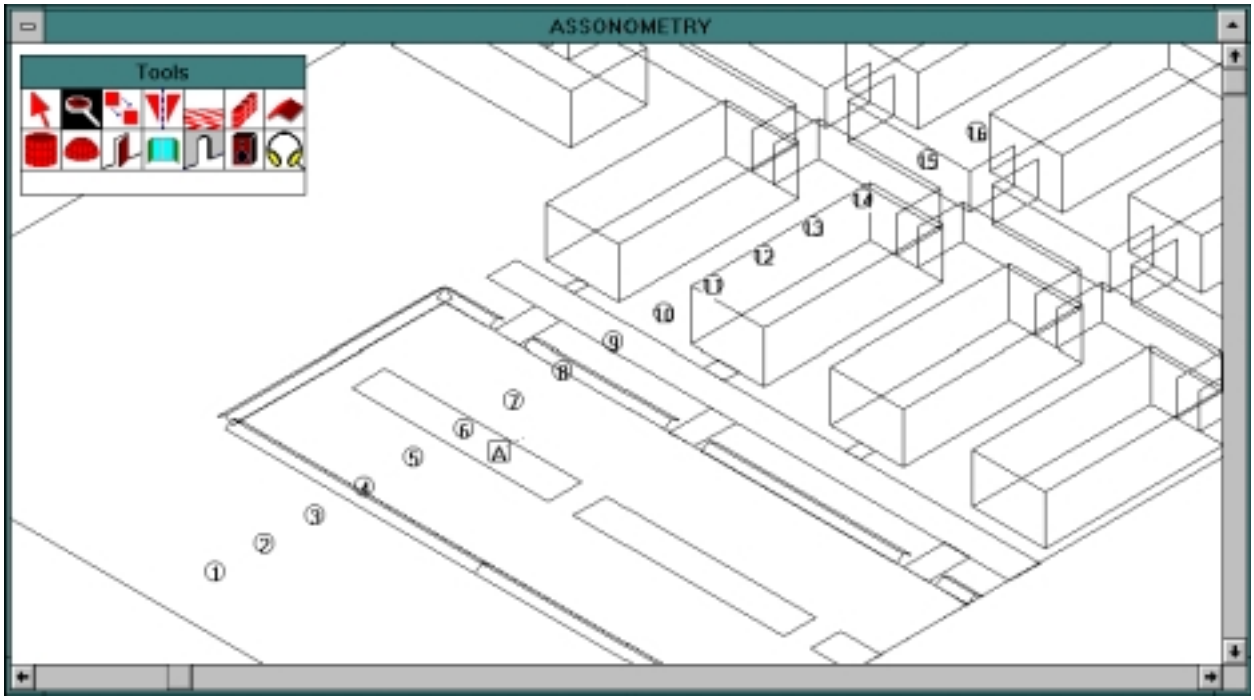

Figure 8 - 3D view of the geometry studied

This test case involves propagation on 2 different kinds of ground (hard asphalt and grass), with embankments having an height of 1m and with buildings 10m and 7m tall. The facades of these buildings are continuous crystal. The source height was 1m, and the microphones were placed at 1.3m over the soil.

In each measurement position a digital recording of 60s of MLS signal was made. Furthermore, another 60s recording without the signal was performed, to verify the background noise level. As the overall sound power level of the loudspeaker was limited (100 dB), in many points the signal felled under the background noise, but it was still possible to measure it thanks to the MLS properties.

4. Comparative results

The experimental results are presented together with the numerical simulations, to make it easy to compare them and to exploit the discrepancies.

Looking at figure 9, it is clear that the Ramsete code gives better results near the source, while the ISO-DIS 9613 is more accurate in the points at larger distance and very shielded from the buildings. This result is quite obvious, as Ramsete manages properly multiple reflections and considers the effective directivity balloon for each of them, but does not include any evaluation of many excess attenuation effects. Furthermore, it seems that ISO-DIS 9613 is more accurate in the evaluation of the shielding effect caused by the buildings, that is overestimated by Ramsete.

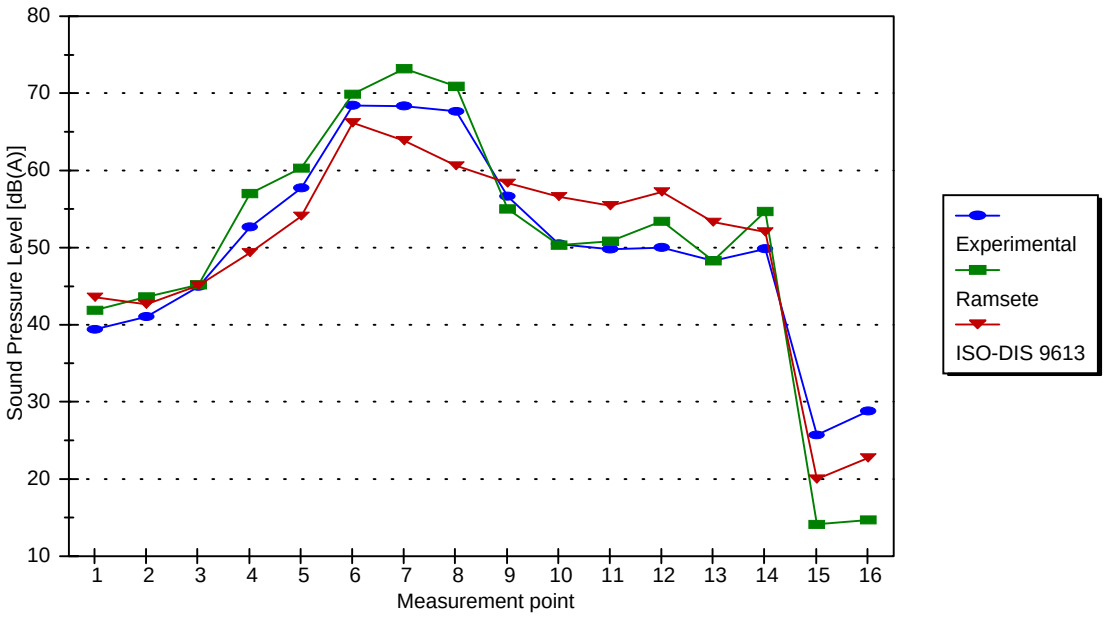

Figure 9 - Comparison of the results in dB(A)

Other interesting things come out observing the spectra in some particular points, as reported in figs. 10 and 11:

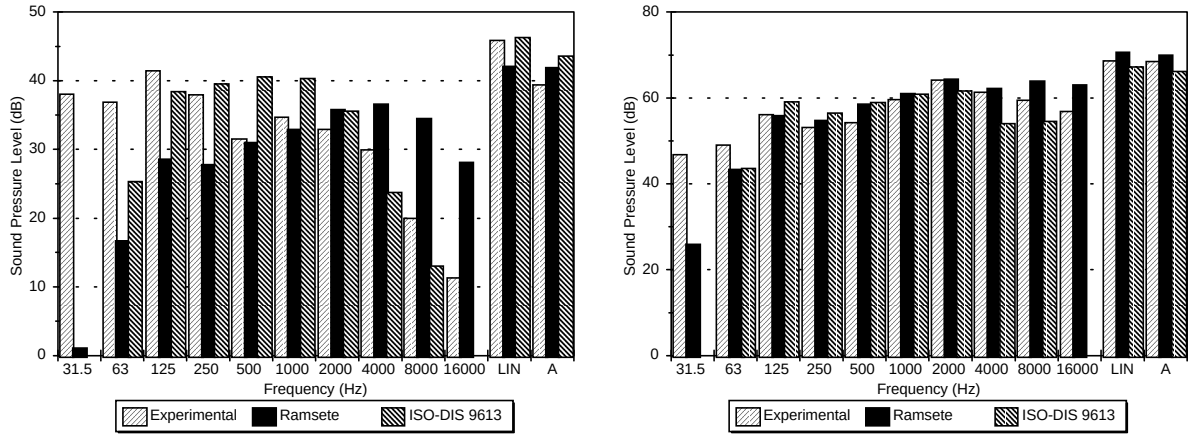

Figure 10 - Spectra at point # 1 (left) and # 6 (right)

It can be observed that in point 1 (behind the source, and partially shielded), the three spectra are quite different: the experimental one exhibits large background noise contamination in the low frequency bands, while Ramsete overestimates the high frequency bands level of more than 10 dB. It is evident at this point that the air absorption formula (eq. 4) is not realistic enough to take into account what it happens on a soft grass soil; this instead seems well modelled by the ISO-DIS 9613 code. Probably also the diffraction effect of screens is not correctly modeled: in fact, the Kurze formula (2) is applied only if the screen intercepts the line connecting the source and the receiver, whilst in this case this does not happen, although the line passes a few centimeters above the embankment. So no edge diffraction is computed by Ramsete in point 1.

But if we look at what happens in point 6 (that is the nearest to the sound source), we find that here the three spectra are very similar: obviously at this little distance the excess attenuation terms are not very important, and the spectra modification is mainly governed by the source directivity.

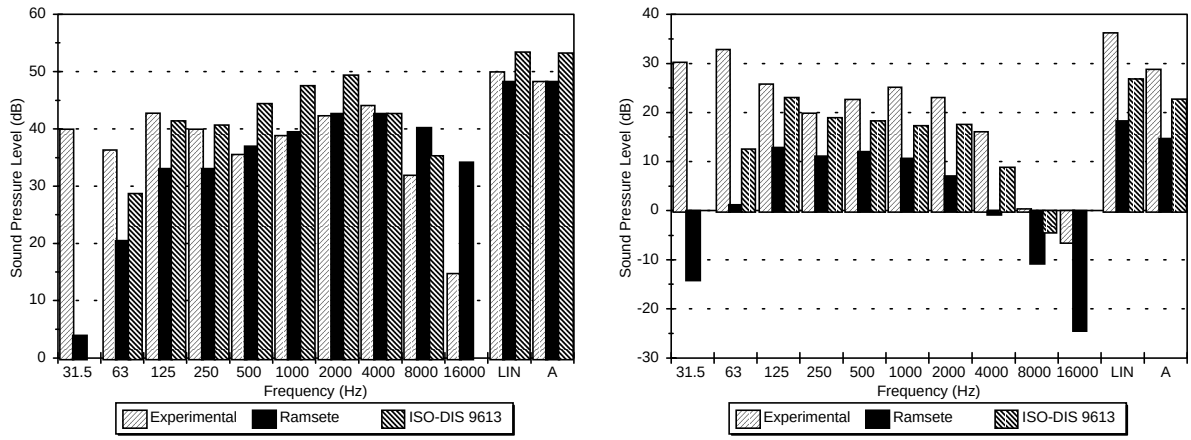

Figure 11 - Spectra at point # 13 (left) and # 16 (right)

The point 13 is between the buildings, were the multiple reflections over the facades are dominant, and still no shielding effect is present; in this case the Ramsete's results are very

similar to the experimental ones, excluding frequency of 125 Hz and below, where the measurements results are clearly affected by the background noise. On the other hand in this point the ISO-DIS 9613 code systematically overestimate the sound levels in all the frequency bands,

The point 16 is behind the buildings, where the shielding effect is very high, and the absolute levels fall to very little values. Here the Ramsete results are widely underestimated, while the Image Source code seems to produce reasonable results, also if there is the doubt that the experimental measurements could be affected by background noise at any frequency; anyway the Signal-to-Noise ratio computed by the MLSSA software indicates that the measurement should be acceptable (S/N > 10 dB) at frequency of 250 Hz and above.

It must be noted that the diffraction formula included in Ramsete (2) was originally developed and tested for thin screens: although Maekawa suggested to use it also in case of thick barriers and double diffractions, it is known that in such cases the attenuation is frequently overestimated.

A simultaneous comparison of the computed and measured results in all the frequency bands and positions is possible with the three graphs of fig. 12.

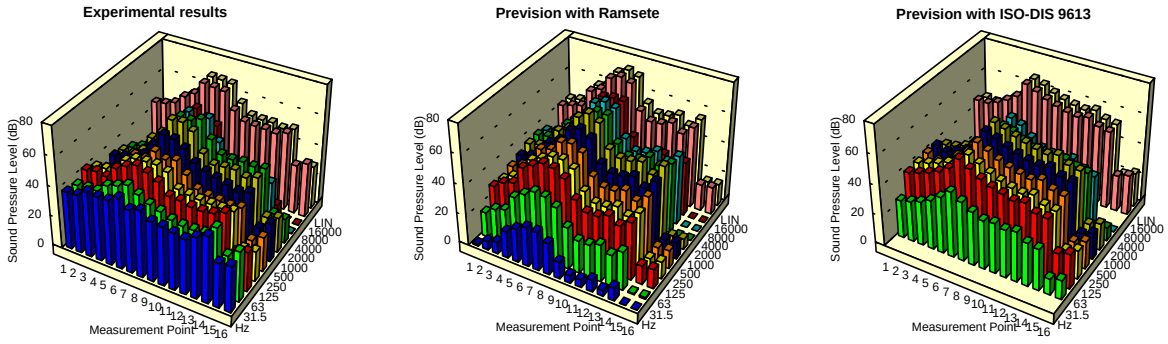

Fig. 12 - Comparison of the spectra in all receiving positions

This picture shows that the results can be seen as a matrix of numbers, where the measurement points are the columns and the frequencies are the rows. A single-number evaluator of the compliance of the two numerically-computed result matrixes can be obtained by computing the square-average of the deviation of each number from the corresponding cell of the experimental matrix. This evaluation produced the following results:

	Ramsete	ISO 9613
Square-averaged error	6.20 dB	5.39 dB

A different way to look at the same information is to build a plot of the numerically computed values versus the experimental ones. The two graphs reported in fig. 13 show such a construction for the two numerical models employed here (Ramsete and ISO9613).

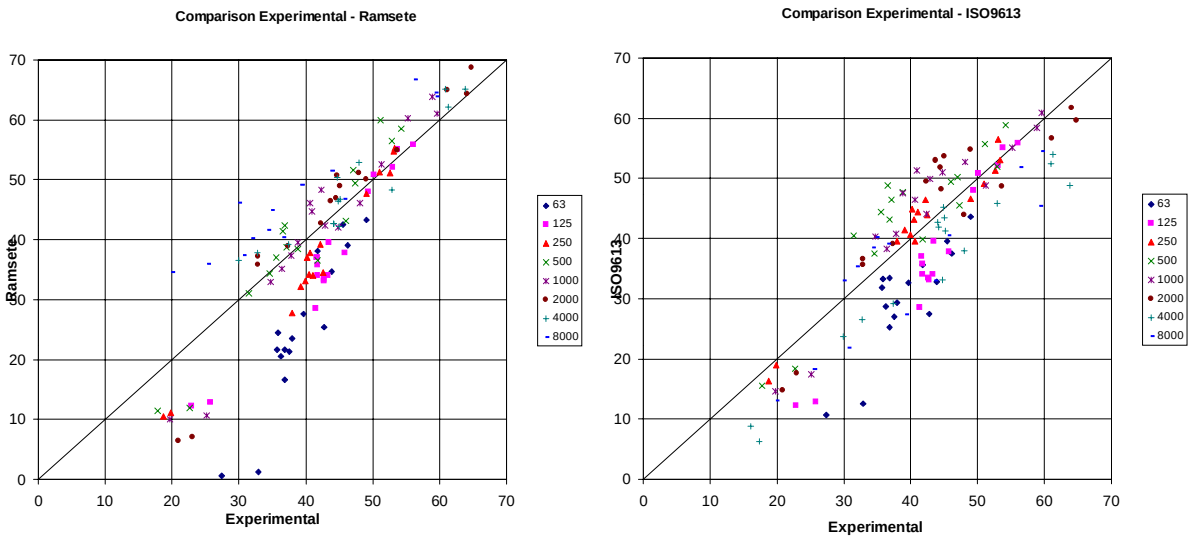

Fig. 13 - Comparison of the numerical/experimental levels

It can be observed that Ramsete has lower error at higher SPL values (which means near the source and at medium-high frequencies), whilst ISO9613 produces almost the same behaviour independent of the absolute SPL. Both programs have larger errors at low frequency, probably because none of them takes into account the wavy phenomena.

Ramsete does not compute just the sound pressure levels, but it also records the impulse response between source and receiver. Thus it is possible to compare it directly with the experimental one, as shown in fig. 14: it can be seen how the principal specular reflections are properly modelled.

On the other hand, the experimental impulse response exhibit broader reflection patterns, caused by sound diffusion (reflection on rough surfaces) and edge diffraction. These phenomena are not properly simulated in the actual version of Ramsete, although the introduction of a surface diffusion effect is planned for the next release. It must be noted that the lack of diffusion in the simulated impulse response, also if not affecting the overall Sound Pressure Level, can cause audible differences while listening directly at the impulse response (after proper translation in wave format) [4].

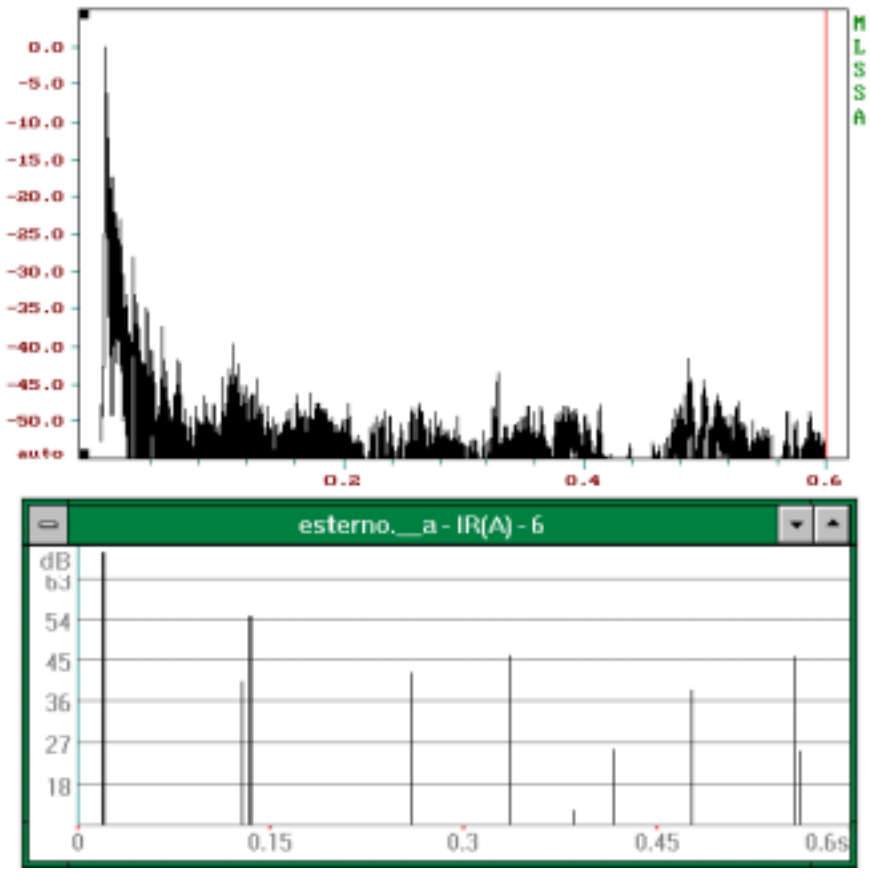

Figure 12 - Comparison between experimental and numerical I.R. - point #6

5. Conclusions

The results show that actually the pyramid tracing implementation available in the Ramsete package is not always accurate for outdoor calculations, as at large source-receiver distances the ground effect and the ray curvature cause some significant differences between experimental results and numerical simulation.

The ISO/DIS 9613 standard suggest computation formula that seem simple and yet accurate enough to enable fast numerical computations, although their direct implementation does not allow easily to take into account other important acoustic phenomena, as multiple reflections on facades. In the prosecution of this work the advanced capabilities of managing excess attenuation contained in the ISO-DIS 9613 shall therefore be added to the pyramid tracing code.

Also the experimental technique, employed here for the first time, resulted very efficient for outdoor measurements: the instrumentation is fully portable and battery operated, no physical link exists between the source and the receiver, the data acquisition is fast and easy, the excitation signal properties allow for a large background noise reduction by synchronous averaging. Furthermore, the MLSSA software enables the computation of almost any kind of acoustic results, and the measured impulse responses can be compared also by listening tests with those obtained by numerical computation, both directly or after convolution with a proper (anechoic) source signal [4].

As a general conclusion, the better accuracy of Ramsete near the source is marginal, as in outdoor noise problems what usually is required is to obtain accurate predictions very far from the sound sources. At this time, simple computation methods based on empirical formulas, such

as ISO9613, appear to be still superior, for outdoor predictions, to computational-intensive prediction schemes, such as ray tracing or pyramid tracing.

Acknowledgements

The software routines, which perform ISO/DIS 9613 calculations, were developed by Luigi Maffei [5], who also worked out the required computations. Paolo Galaverna and Guido Truffelli are acknowledged for substantial contribution to the development of the Ramsete package.
This work was partially supported by the Italian CNR grant # 95.00463.CT12.

References

[1] Farina, A. RAMSETE - a new Pyramid Tracer for medium and large scale acoustic problems, *Proc. of Euro-Noise 95*, Lyon, France 21-23 march 1995, Vol. I p. 55.

[2] Farina, A. Pyramid Tracing vs. Ray Tracing for the Simulation of Sound Propagation in Large Rooms, in COMACO95, *Proc. of Int. Conf. on Computational Acoustics and its Environmental Applications*, Southampton, England, 1995, Computational Mechanics Publications, Southampton 1995, p. 109.

[3] Farina A. Verification of the accuracy of the Pyramid Tracing algorithm by comparison with experimental measurements of objective acoustic parameters, *Proc. of ICA95*, Trondheim, Norway, 26-30 June 1995, vol. II p. 445.

[4] Farina A. Auralization software for the evaluation of the results obtained by a pyramid tracing code: results of subjective listening tests, *Proc. of ICA95*, Trondheim, Norway, 26-30 June 1995, vol. II p. 441.

[5] Farina A., Maffei L. Sound Propagation Outdoor: Comparison between Numerical Previsions and Experimental Results, in COMACO95, *Proc. of Int. Conf. on Computational Acoustics and its Environmental Applications*, Southampton, England, 1995, Computational Mechanics Publications, Southampton 1995, p. 55.

[6] Farina A. An example of adding spatial impression to recorded music: signal convolution with binaural impulse responses, *Proc. of "Acoustics and Recovery of Spaces for Music"*, Ferrara (Italy) 27-28 Oct. 1993, p. 36.

[7] Farina A. Previsione del rumore in ambiente di lavoro a partire dai dati di potenza sonora, *Atti del Convegno "Rumore e Vibrazioni: Certificazione delle Macchine"*, Modena (Italy) 2-3 dicembre 1993, p. 141.

[8] Lewers T. A combined Beam Tracing and Radiant Exchange computer model of room acoustics, *Applied Acoustics*, Vol. 38 no.s 2-4 (1993), p. 161.

[9] Kurze, U.J. Noise Reduction by Barriers, *Journ. of Ac. Soc. America*, vol. 55 (1974), pp. 504-518.

[10] Attenborough K. Review of Ground Effects on Sound Propagation *Applied Acoustics*, vol. 24 (1988).

[11] Chu, W.T. Impulse Response and Reverberation Decay Measurements Made by Using a Periodic Pseudorandom Sequence, *Applied Acoustics*, vol. 29 (1990), pp. 193-205.

[12] Chu, W.T. Time-variance effect on the application of the M-sequence correlation method for room acoustical measurements, *Proc. of ICA95*, Trondheim, Norway, 26-30 June 1995, Vol. IV, p. 25.